Electronic Supplementary Material (ESI) for Journal of Materials Chemistry

Figure of merit of nanoparticle scintillators regarding the PDTX application

The efficiency of a functionalized nanoscintillator material (FNM) in a PDTX application can be judged by its capability to generate singlet oxygen after its deposition in desired target cells and under given irradiation conditions. Under common irradiation doses the requirements on the necessary efficiency of this process has been estimated to be very high to achieve sufficient cytostatic effect, so called „Niedre killing dose“ [A1].

Figure of merit (FoM) of a FNM can be defined in a most simple form as

$$\mathrm{FoM} = \mathrm{ACX} \cdot \mathrm{SE} \cdot \mathrm{OI} \tag{1}$$

where the first, second and third parameter in eq. 1 express the capability of a FNM to attenuate the incoming X-ray irradiation (ACX), to convert its deposited energy into scintillation photons (excited states of emission centers) (SE) and to transfer the energy of these photons (excited states) to the functionalized organics at the nanoparticle surface (OI), respectively, to generate singlet oxygen. Such a definition enables the relative comparison of all the compounds regarding their theoretical performance in a PDTX application and show the importance of three critical cotributing processes in it. ACX is the attenuation coefficient of FNM for the X-rays used for irradiation which is given by the nanoscintillator density ρ and effective atomic number Z_{eff}. For X-rays up to 200 keV energy the photoeffect is the dominant interaction betweeen the radiation and matter and ACX becomes [A2,A3]

$$\mathrm{ACX} \propto \rho \cdot Z_{\mathrm{eff}}^{4} \tag{2}$$

Scintillation efficiency SE is usually defined as a number of scintillation photons produced per 1 MeV of the absorbed energy and can be written as

$$\mathrm{SE} = \frac{10^{6} \cdot S \cdot Q}{\beta \cdot E_{\mathrm{g}}} \tag{3}$$

where $\beta \cdot E_{\mathrm{g}}$ is the energy necessary for the production of one electron-hole pair (β is conversion coefficient and E_{g} is the bandgap value in eV). Typical values of β are about 3, 2-3 and 1.5-2 for strongly covalent semiconductors, oxides with ionic-covalent bonding and strongly ionic (fluorides) compounds, respectively [A4]. S is transfer efficiency related to delivery of produced electrons and holes to the emission centers and Q is quantum efficiency of the emission center itself [A5]. The parameter Q can be easily measured from temperature dependence of photoluminescence decay times and intensities and is close to 1 for the most of emission centers considered here. The parameter S can vary considerably even for the same material prepared by different technological routes due to different material defects and energy traps introduced by a particular technology. For our purpose we consider both $S = Q = 1$, i.e. we provide the upper theoretical limit of scintillator efficiency $\mathrm{SE}^{\mathrm{theor}}$ given as a number of generated electron-hole pairs (giving rise to an equal number of scintillation photons).

Overlap integral (OI) is defined as the integral of the product of the normalized nanoscintillator emission spectrum $I(\lambda)$ and the porphyrin compound absorption spectrum $A(\lambda)$

$$\mathrm{OI} = \int I(\lambda) \cdot A(\lambda)\, \mathrm{d}\lambda \qquad (4)$$

and quantifies the probability of energy transfer (both radiative and nonradiative) from nanoscintillator particle to the surface-residing porphyrin.

Table 1 – List of compounds and the values of respective parameters which are important for quantitative evaluation of their Figure of Merit FoM regarding PDTX applications. E_g, ρ, λ_{em}^{peak}, τ_{em} stand for material bandgap, density, emission maximum and luminescence decay time values, respectively, see also the text for explanations. Data from Refs. A3-A26.

Compound	E_g [eV]	ρ [gcm^{-3}]	ρZ_{eff}^4 x 10^6	λ_{em}^{peak} [nm]	τ_{em} [µs]	SE^{theor} [phot/MeV]	OI	FoM x 10^3
CdTe	1.44	6.2	39	500-800	<0.01	224000[A4]*	1.0	8740
CdSe	1.74	5.8	20	600-700	0.001	191000	0.9	3440
CdS	2.42	4.82	17	500-660	0.01-0.04	138000[A4]*	1.5	3520
ZnS:Ag$^+$	3.91	4.09	1.9	450	~1	171000[A4]*	9.7	3150
ZnS:Mn^{2+} (Eu^{2+})	3.91	4.09	1.9	590 (610)	500-3000	171000[A4]*	1.5 (1.1)	490 (357)
ZnO	3.34	5.6	3.0	385	0.001	143000[A4]*	9.2	3950
TiO_2	3.2	4.23	0.39	400-420	n.r.	104000	34	1380
Gd_2O_2S:Tb^{3+}	~5	7.32	85	545	600	80000	1.9	12900
$Lu_4Hf_3O_{12}$: Tb^{3+} (Eu^{3+})	5.5	9.04	170	540 (610)	3200 (3000)	72700	1.9 (1.3)	23500 (16100)
$Lu_3Al_5O_{12}$: Ce^{3+} (Pr^{3+})	~8	6.7	75	510 (310)	0.06 (0.02)	50000	5.8 (10)	21800 (37500)
BaFBr:Eu^{2+}	8.2	~5.1	23	390	0.8	48800	12.4	13900
CeF_3	~10.4	6.16	39	280-310	0.02-0.04	42000	9.5	15600
LaF_3:Tb^{3+}	~10.4	5.9	34	545	2500	56500	1.9	3650
LaF_3:Ce^{3+}	~10.4	5.9	34	280-310	0.02-0.04	56500	7.4	14200
CaF_2:Ce^{3+}	12.2	3.2	0.22	310-340	0.06-0.15	48200	5.5	58
CaF_2:Eu^{2+} (Mn^{2+})	12.2	3.2	0.22	425 (500)	0.7 (20000)	48200	7.2 (3.7)	76 (39)
LuF_3:Ce^{3+}	~10.3	8.3	130	310	0.02	57100	7.4	54900
SiO_2 (am.)		2.2	0.03					

n.r. ...not reported, * values of parameter β were taken from [A4] for this compound

The example of the absorption spectrum of hematoporphyrin „D“ (used in the approved PDT drug “Photofrin”) dissolved in tetrahydrofuran is displayed in Fig. 1 together with emission spectrum of a scintillator and calculated product of spectra. In Table 1, there are OI values calculated according eq. (4) using known emission spectra of each scintillator material or their approximation. All the characteristics, calculated parameters and resulting FoM are in Table 1.

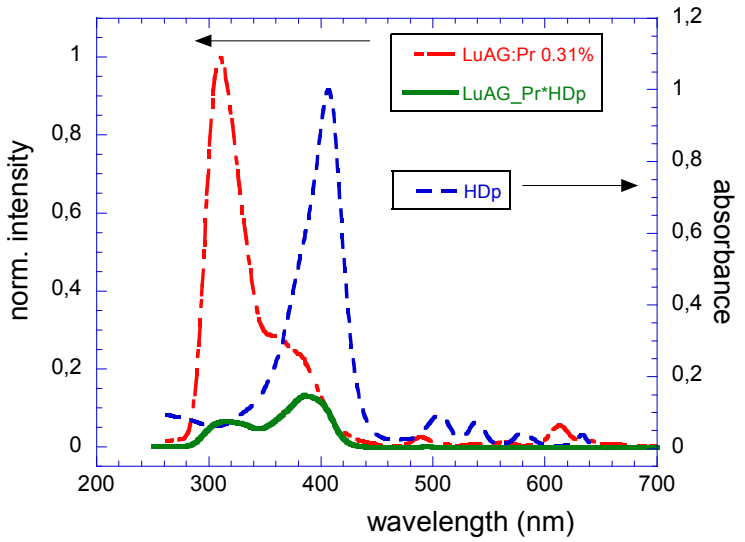

Fig. 1 – Normalized LuAG:Pr radioluminescence and hematoporphyrin „D“ (HDp) absorbance spectra and the product of these two spectra used in eq. (4).

Compounds in Table 1 were indicated as possible candidates for PDTX in [A6-A13] and refs therein. Typical strongly covalent semiconductors with small direct bandgap, namely CdTe, CdSe and CdS are mostly prepared in the form of quantum dots (QD) with the size below 10 nm. They show high theoretical limit of scintillator efficiency, medium-lower values of attenuation coefficient and emission in the yellow-red part of the spectra which does not suit perfectly to the absorption spectrum of porphyrins in Fig. 1, i.e. the value of the overlap integral OI can be lower as well. Though very high quantum efficiency of photoluminescence is often mentioned in literature, their radioluminescence intensity under X-ray excitation has been shown rather weak or even absent [A14] which is presumably due to surface-related charge carrier capture and resulting nonradiative recombination. Core-shell technology is often used, where the outer part of QD is formed by a wider bandgap stable compound as LaF_3 [A14] or SiO_2 [A15] which stabilizes the surface of the inner core and even contribute further by an energy transfer to an increased scintillation efficiency of such composite QD. However, due to lower attenuation coefficient especially in the case of SiO_2 shell, see Table 1, and a physical separation of the scintillation core and porphyrin acceptor at the QD surface, which will certainly decrease the contribution of nonradiative part of the energy transfer process, such a strategy may not be optimal. The other

reasons why such strategy is used is also to get rid of the risk of toxic cadmium penetration to the organism in PDT application itself.

ZnS-based materials are known as the most efficient X-ray powder phosphors [A5] and ZnS:Ag has also suitably positioned emission spectrum with respect to dominant absorption peaks of porphyrins. However, very small attenuation coefficient considerably decreases its figure of merit. Furthermore, stability of this material in a biological environment is also questionable.

It is not clear, why TiO_2 has been mentioned as a possible candidate for PDTX [A6]: even the latest ultrasmall TiO_2 QDs show quantum efficiency of photoluminescence as small as 2% [A16]. Consequently its SE falls down to 5000 phot/MeV and its very small attenuation coefficient (cf. Table 1) makes it completely unsuitable.

Very fast Wannier exciton emission of undoped ZnO around 380-390 nm is suitably positioned with respect to porphyrin absorption bands in Fig. 1. However, under X-ray excitation the ZnO nanoparticles usually show the dominant light output in the green-red part of the spectrum due to the defect-related emission [A17]. Ga-doped ZnO powders with an optimized post-preparation heat treatment in reduction atmosphere [A18] have shown an extreme enhancement of the excitonic emission even under X-ray or gamma ray excitation and were indicated as promising ultrafast scintillator. However, its low attenuation, see Table 1, does not make it too perspective for PDTX application.

Gd_2O_2S based phosphors known for a long time [A19] found their commercial application in CT medical imaging [A20]. The best performing Tb-doped and Pr-doped Gd_2O_2S show dominant narrow emission lines at about 545 nm and 400 nm, respectively, which might be critical in matching the absorption spectra of porphyrins. So far, to our knowledge, there is also no report truly showing nanomorphological character of this material. Nevertheless, in principle it could show favourable FoM values with well-matched functionalized organics due to excellent attenuation coefficient and proved high scintillation efficiency in micrometric powder and optical ceramic forms.

Interestingly, high density oxide compounds have not been mentioned much so far regarding PDTX application though quite some of them are known as very efficient bulk scintillators which are successfully employed in a number of applications [A5,20]. Recently, ultrahigh density $Lu_4Hf_3O_{12}$-based scintillating powders have been reported and mentioned in this respect [A13,21]. In this paper we draw the attention to Ce or Pr-doped $Lu_3Al_5O_{12}$ with highly favourable combination of all three parameters defining FoM in eq. (1). This is thanks to broad emission bands based on 5d-4f transition of Ce^{3+} and Pr^{3+} dopants (these emissions are quenched in $Lu_4Hf_3O_{12}$ host due to positioning of 5d level of dopants in conduction band [A21]). Especially in the latter the overlap integral is much higher with respect to $Lu_4Hf_3O_{12}$-based nanoscintillator. Moreover, practical scintillation efficiency of these two materials can be compared as the radioluminescence spectra measurements of their powders with respect to a scintillation standard

are available from the same laboratory, Fig. 2 below and Fig. 6 in the paper. Spectra integrals can serve as a measure of scintillation efficiency of a given material. The value of spectrum integral of $Lu_3Al_5O_{12}$:Ce0.2% is about 25 times higher than that of Tb or Eu-doped $Lu_4Hf_3O_{12}$.

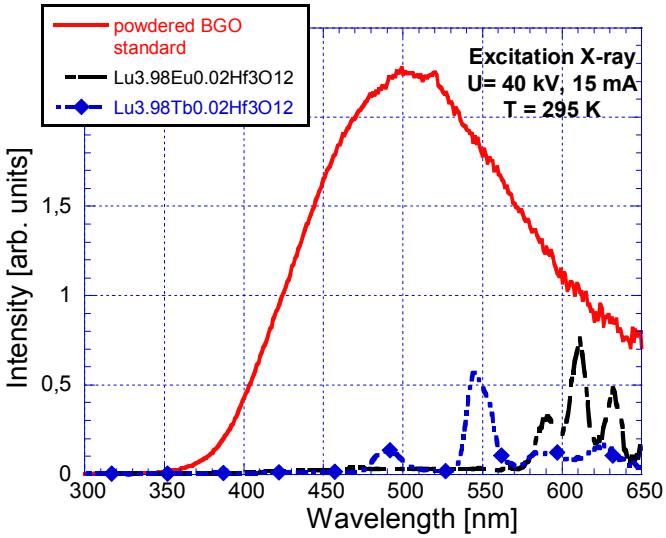

Fig. 2 – Radioluminescence spectra of the Eu and Tb-doped $Lu_4Hf_3O_{12}$ [A21] and a powdered BGO standard sample. Spectra can be compared in an absolute manner.

In the group of fluoride materials, not too high attenuation factor values are calculated for BaFBr, CeF_3 and LaF_3 materials, extremely small value is obtained for CaF_2, and the only perspective material in this respect is the Ce-doped LuF_3. The reported values of scintillation light yield for single crystals are about 8000 phot/MeV for LuF_3:Ce [A22], while 26 000 phot/MeV were obtained for $Lu_3Al_5O_{12}$:Ce [A23] and up to 20 000 phot/MeV for $Lu_3Al_5O_{12}$:Pr [A24] so that real SE in the latter two LuAG-based scintillators is expected to be 2-3 times higher compared to LuF_3:Ce. Moreover, though the mentioned binary fluoride materials are stable in air, it is not clear, how long they can resist in nanoparticle form in a biological environment, while the stability of the above mentioned oxide materials is by far much higher in this respect.

To conclude, using the above derived figure-or-merit of PDTX-considered nanoscintillators, the highest intrinsic performance is found for LuF_3:Ce, $Lu_3Al_5O_{12}$:Ce(Pr) and $Lu_4Hf_3O_{12}$:Tb. Taking into account the practical scintillation performance reported in literature for some of these materials and the current status of their production in nanoparticle form, the $Lu_3Al_5O_{12}$-based materials show the best prospectives.

Literature

A1. N. Y. Morgan et al, Radiat. Res. 2009, **171,** 236.

A2. P. A. Rodnyi, Physical processes in inorganic scintillators. CRC press, New York 1997, pp. 11-15.

A3. C. W. E. van Eijk, Nucl. Instrum. Methods Phys. Res. 2001, **460**, 1.

A4. P. A. Rodnyi, P. Dorenbos, C. W. E. van Eijk, Phys. Status Solidi B 1995, **187**, 15.

A5. M. Nikl, Meas. Sci. Technol. 2006, **17**, R37.

A6. J. Takahashi and M. Misawa, Nanobiotechnol. 2007, **3**,116.

A7. Y. Liu, W. Chen, S. Wang, A. G. Joly, Appl. Phys. Lett. 2008, **92**, 043901.

A8. E. Abliz, J. E. Collins, H. Bell, D. B. Tata, J. X-Ray Sci. Technol. 2001, **19**, 521.

A9. W. Chen, J. Biomed. Nanotechnology 2008, **4**, 369.

A10. W. Yang et al., Int. J. Radiat. Oncol. Biol. Phys. 2008, **72**, 633.

A11. W. Chen and J. Zhang, J. Nanosci. Nanotechnol. 2006, **6**, 1159.

A12. P. Juzenas et al., Adv. Drug Delivery Rev. 2008, **60** 1600.

A13. A. Lauria et al., J. Mater. Chem., 2011, **21**, 8975.

A14. M. Hossu, et al, Appl. Phys. Letters 2012, **100**, 013109.

A15. P. Yang, M. Ando, N. Murase, Langmuir 2011, **27**, 9535.

A16. S. Kaniyankandy and H. N. Ghosh, J. Mater. Chem. 2009, **19**, 3523.

A17. T. Gbur, et al, J. Nanoparticle Res. 2011, **13** 4529.

A18. E. D. Bourret-Courchesne, S. E. Derenzo, M. J. Weber, Nucl. Instrum. Methods Phys. Res. A 2009, **601**, 358.

A19. L. H. Brixner, Mater. Chem. Phys. 1987, **16** 253.

A20. C.W.E. van Eijk, Phys. Med. Biol. 2002, **47** R85.

A21. L. Havlak, et al, Opt. Mater. 2010, **32** 1372.

A22. B. Moine et al, Mat. Sci. Forum 1997, **239-241**, 245.

A23. C. Dujardin, et al, J. Appl. Physics 2010, **108,** 013510.

A24. K. Kamada,et al, J. Cryst. Growth (2012). doi:10.1016/j.jcrysgro.2011.11.079

A25. S. Shionoya, W.M. Yen, Phosphor handbook. CRC press, New York 1998.

A26. W.M. Yen, M.J. Weber, Inorganic Phosphors.CRC press, New York 2004.